Received 17 March 2023; revised 8 April 2023; accepted 10 April 2023. Date of publication 14 April 2023; date of current version 27 April 2023.
Digital Object Identifier 10.1109/OJAP.2023.3267299

A Concept of Advanced Design Governed by Theoretically Predicted Current Distributions on the Ground Plane Beneath an Aperture-Fed Microstrip Antenna

DEBI DUTTA [1] (Graduate Student Member, IEEE), DEBATOSH GUHA [1] (Fellow, IEEE), AND CHANDRAKANTA KUMAR [2] (Senior Member, IEEE)

[1] Institute of Radio Physics and Electronics, University of Calcutta, Kolkata 700009, India

[2] Department of Space (Govt. of India), U R Rao Satellite Centre, Bengaluru 560017, India

CORRESPONDING AUTHOR: D. GUHA (e-mail: dguha@ieee.org)

This work was supported in part by the Abdul Kalam Technology Innovation Fellowship of Indian National Academy of Engineering (INAE) and in part by the Department of Science and Technology–Science and Engineering Research Board (DST-SERB), Government of India.

ABSTRACT This work addresses a concern of aperture coupled microstrip patch which is commonly overlooked. Such feeding configuration is typically believed to be immune to high cross-polar (XP) radiations, which indeed is a paradox. It actually offers considerably low XP only across H-plane, but concerning high XP over its diagonal or skewed planes (azimuth ≈ 45°-70°). An aperture feed, therefore, hardly reveals any advantageous feature in terms of the overall XP discrimination. Such a major shortcoming of aperture-fed microstrip, to the best of our knowledge, has been addressed and successfully resolved in this article for the first time. It explores a way of mitigating near field issues based on theoretical analysis and has proposed a simple strategic approach to reform the same for a rectangular patch. A representative design, theoretical justification, and experimental studies with an S-band prototype have been presented. XP suppression by 11dB has been experimentally achieved in the diagonal (D-) plane with no considerable changes in its H- or E-plane. That eventually attains an overall XP discrimination by nearly 27dB from the perspective of 3D radiation scenario. The proposed technique hardly affects the co-polar radiations or gain of its traditional design. Moreover, this is satisfactorily functioning for a 2×2 sub-array with a remarkable co-to-cross isolation by about 34dB over the entire radiation planes.

INDEX TERMS Cross-pol (XP) suppression, diagonal plane, ground plane shaping, microstrip antenna.

I. INTRODUCTION

THE MICROSTRIP antenna community started realizing the significance of cross polarized (XP) radiation and its accurate estimation when Hansen [1], Huynh et al. [2], and Lee et al. [3] initiated the analytical studies. Their analyses identified the orthogonal modes as the XP sources and systematically quantified them as functions of azimuth angle φ indicating the minimum occurring at $\varphi \approx 0^0$, maximum around $\varphi \approx \pm 45^0$ and moderate values near $\varphi \approx 90^0$. As a result, the cross polar discrimination (XPD) bears a minimum value over the skewed region spanning over $\varphi \approx 45°$ - $70°$.

Till date, several XP reduction techniques have been explored which primarily addressed and tried to weaken the orthogonal modes as a remedial measure. Structurally they are categorized as (i) planar techniques comprising balanced feed [5], [6], [7], electromagnetic bandgap (EBG) [8], [9] and defected ground structures (DGSs) [10], [11], [12], and (ii) non-planar techniques which embody various perturbations including thick and vertically erected ground plane (GP) [13], [14], and inserted vertical pins [15], [16], [17]. But noticeably each of them could control the XP over H-($\varphi \approx 90°$) plane only.

Very recently, a few investigations have tried to address the D-plane issues [18], [19], [20], [21]. The work in [18] dealt with theory only without any attempt of minimizing it. The studies in [19], [20], [21] demonstrated some degree of improvements for standalone probe-fed patches by introducing defects on the ground plane and as such none of these were found suitable to accommodate corporate feeds required for the array configurations.

The present investigation addresses a different engineering concern that relates to the aperture-fed version of a microstrip patch. It is commonly known for its lowest XP feature [22], [23] but that is true only over $\varphi = 90°$ plane. Consistent high XP level remains alarming over the D- plane (around $\varphi = 45°$). This work, to the best of our knowledge, addresses the above concern based on a theoretical understanding and proposes a simple commercially viable solution for the first time. The analysis reveals that, besides the orthogonal modes, near magnetic field components such as H_X and/or H_Y also play vital roles in contributing to the XP radiations over the φ planes. This knowledge has been explored in optimizing the favorable near field components which are caused by the surface conduction currents. Removal of conduction currents around the ground plane (GP) corners has been identified and executed in the present study. But the actual solution is not straight forward at all. It needs further consideration of introducing compensatory current paths which have been thoroughly studied in steps.

The final outcome appears a fully planar GP with strategic shaping. This is commercially viable and promises overall XP reduction by 14 dB over the skewed planes and about 7 dB across the so called H-plane. Most significantly, the engineered ground hardly causes any change in the primary radiation or gain values. A thorough comparison with respect to the earlier endeavor has been presented.

The proposed idea has further been examined for an array of elements. A representative sample of 2×2 aperture coupled array with corporate feed bearing identical ground plane engineering has been demonstrated with a promise for 12dB reduction in XP level over the skewed or D-plane. That in turn results in overall 3D co-to-cross isolation around 34dB.

This method is straightforward, planar, and does not incorporate any additional structures. The final product is easy to fabricate and cost effective. Moreover, it allows adequate flexibility in the design based on the primary element shape and size. Utilizing the concept in array may find a possible scope for further exploration because D-plane rectification is indeed a challenge in view of a key need of adaptive arrays that requires wide three-dimensional (3D) signal coverage throughout the entire azimuth plane [24], [25], [26].

II. THEORY AND ANALYSIS

The proposed design has been guided with the help of theoretical interpretation about the XP controlling factors as a function of GP currents and its associated magnetic fields in the substrate. Total radiation fields due to a microstrip patch is contributed by two sources: (i) equivalent magnetic current source across the radiating aperture, and (ii) the induced current on the finite ground [27], [28]. This leads to the instantaneous near-field as [28]:

$$\boldsymbol{E(\theta, \varphi) \equiv E_G(\theta, \varphi) + E_P(\theta, \varphi)} \tag{1}$$

where, E_G (θ, φ) and E_P (θ, φ) are near electric fields contributed by ground and patch currents respectively. Since our aim is to investigate the contribution of the GP only, (1) can be written exclusively:

$$\begin{aligned} E(\theta) &\equiv E_G(\theta) = -j\omega\mu\epsilon\ A_G(\theta) \\ E(\varphi) &\equiv E_G(\varphi) = -j\omega\mu\epsilon\ A_G(\varphi) \end{aligned} \tag{2}$$

where A_G (θ, φ) represents the magnetic vector potential derived from GP current sources (J_S) and can be expressed as:

$$\mathbf{A_G} = \frac{\mu}{4\pi} \iint_{-\frac{x}{2},-\frac{y}{2}}^{\frac{x}{2},\frac{y}{2}} J_S(x, y) \frac{e^{-jkR}}{R} dS' \tag{3}$$

It splits into two parts in the Cartesian coordinate as

$$\begin{aligned} \mathbf{A_G}(\theta) &= \frac{\mu}{4\pi}\frac{e^{-jkr}}{r} \iint J_S\ (x, y)\left(\cos\theta\cos\varphi\ \hat{i} + \cos\theta\sin\varphi\hat{j}\right) dx\, dy \\ &\& \\ \mathbf{A_G}(\varphi) &= \frac{\mu}{4\pi}\frac{e^{-jkr}}{r} \iint J_S\ (x, y)\left(-sin\varphi\hat{i} + \cos\varphi\hat{j}\right) dx\, dy \end{aligned} \tag{4}$$

As one can represent $J_S(x, y) = J(x)\hat{i} + J(y)\hat{j}$, (4) takes the form as:

$$\begin{aligned} \mathbf{A_G}(\theta) &= \frac{\mu}{4\pi}\frac{e^{-jkr}}{r} \iint\left(J_x\cos\theta\cos\varphi + \ \cos\theta\sin\varphi\hat{j}\right) dx\, dy \\ &\& \\ \mathbf{A_G}(\varphi) &= \frac{\mu}{4\pi}\frac{e^{-jkr}}{r} \iint\left(-J_x sin\varphi\hat{i} + \cos\varphi\hat{j}\right) dx\, dy \end{aligned} \tag{5}$$

Ludwig's 3rd definition [29] provides cross-polarized radiation employing only ground plane contribution as

$$XP(\theta, \varphi) = \ E_G(\theta)cos\varphi\ - E_G(\varphi)sin\varphi \tag{6}$$

Which with the help of (2) - (4) helps in estimating XP over $\varphi = 45°$ (D-plane) and 90° (H-plane):

$$\begin{aligned} XP(\theta)_{\varphi=45} &\propto \iint\{J(y)[1 + \cos\theta] \\ &\quad - J(x)[1 - \cos\theta]\} e^{j\beta\acute{r}.\hat{r}} d\acute{s} \\ XP(\theta)_{\varphi=90} &\propto \iint 2J(y) e^{j\beta\acute{r}.\hat{r}} d\acute{s} \end{aligned} \tag{7}$$

Again, Js is related to its source, the near magnetic field H which manifests the signature of GP conduction current as:

$$J_S(x) = \hat{\mathbf{n}} \times H_y \quad \& \quad J_S(y) = \hat{\mathbf{n}} \times H_x \tag{8}$$

$\boldsymbol{n}$ being unit vector normal to GP surface.

TABLE 1. Requirement for the source fields to reduce.

XP Source and Impact on Different φ - Planes: Sources	Impact	Possible way of controlling
(i) H_Y↑ (J_X HIGH)	$XP_{(\varphi\sim45)}$↓	ENHANCE X-POLARIZED GP CURRENT (J_X)
(ii) H_X↓ (J_Y LOW)	$XP_{(\varphi\sim90)}$↓	REDUCE Y-POLARIZED GP CURRENT (J_Y)
(iii) H_Y↑ AND H_X↓ (J_X HIGH & J_Y LOW)	$XP_{(\varphi\sim45\,\&\,90)}$↓	ENHANCE J_X AND OBSTRUCT J_Y

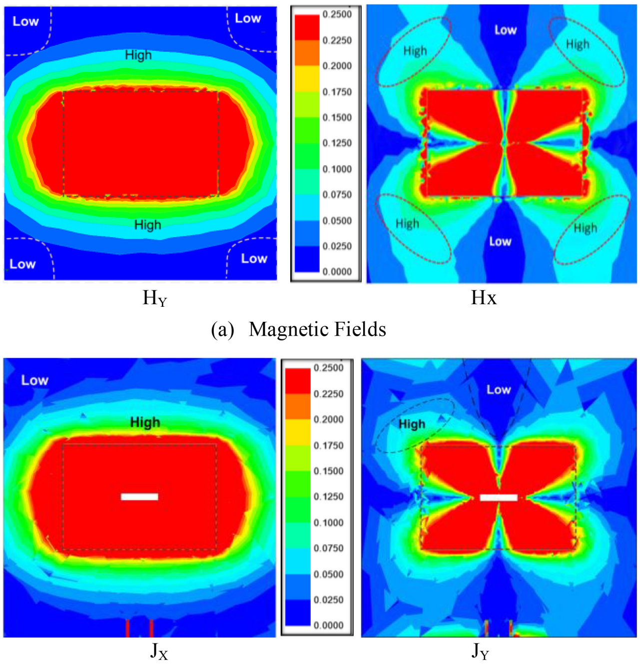

FIGURE 1. Simulated magnitude portrays of a conventional aperture-fed rectangular patch using [30], (a) near magnetic fields (H_Y, H_X) extracted on upper surface of substrate (b) GP conduction current density (J_X, J_Y). Both (a) and (b) follows same scale (0-0.25 A/m), red indicates highest and blue is the weakest magnitude.

The theory indicates higher J_X (& H_Y) in (7) (& (8)) should results in lower XP over the D-pane. Lower J_Y (& H_X) values should also help in reducing XP in both D- and H-planes. Interestingly, a strategic increment of J_X can successfully dominate the influence of J_Y in the structure. This has been shown explicitly in Table 1.

III. CONCEPT BUILDING AND DESIGN

A. DESIGN INSIGHT: GP CONFIGURATION – I

We, therefore, address case (i) in Table 1 and primarily focused on enhancing the source field H_Y. Simulated portrays in Fig. 1 reveal the identical patterns of H and J_S. Both H_Y and J_X are noticeably low around the GP corners of a conventional aperture-fed patch antenna. In contrary, H_X (also J_Y) appears high towards the corner region, which according to conditions (ii) and (iii) of Table 1 preferably need to be low. Therefore, one may recommend removal of GP corner metal beneath the substrate to get rid of low H_Y (unfavorable) and high H_X (unfavorable). Then one may surmise a modified or favorable geometry as shown in Fig. 2. It improvises the GP corners and transforms it to a rhombic-like shape. Henceforth, we examine the modified surface currents for a representative unit that operates in S-band.

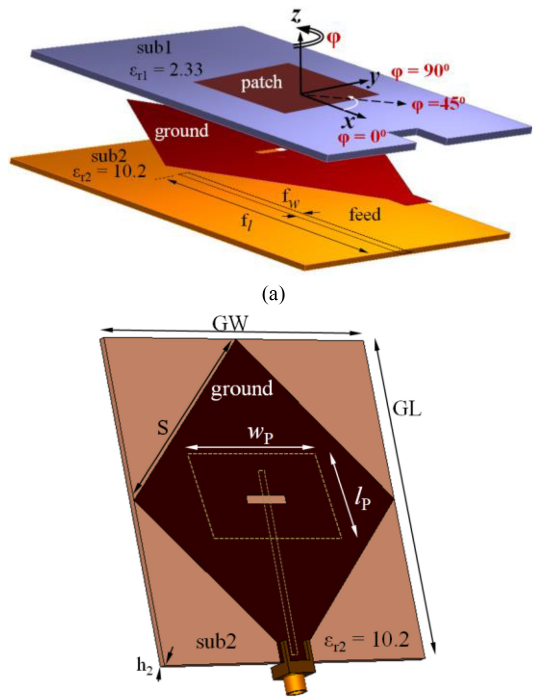

FIGURE 2. Proposed aperture-fed rectangular patch (a) isometric view (layer extracted) (b) new GP configuration-I. Parameters as in Table 2.

TABLE 2. Antenna parameters / dimensions (mm).

Single Unit		Array	
GL	80	GL_a	140
GW	80	GW_a	140
s	53.03	b	28
k	5	S_a	71.55
f_L	50	d_a	5.4
f_W	1.5	a	6
l_S	2	l_{sa}	2
w_S	12	w_{sa}	15
d	2.5	d_1	58
h_1	1.575	d_2	18.5
h_2	1.27	d_3	9.6
l_P	30	d_4	28
w_P	45	d_5	10.2
		d_6	24.3
		k_a	38.8
		L	30
		W	45

Fig. 3 portrays the surface currents components and provides some useful information of GP configuration-I.

(*a*) Compared to Fig. 1(b), 'Low J_X' area has been significantly reduced in Fig. 3 (a). Thus, it supports condition (i) of Table 1 favorably.

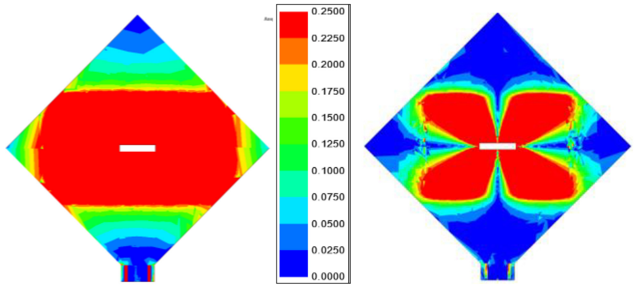

(a) J_X (b) J_Y

FIGURE 3. Simulated portrays of surface current (J_S) in GP configuration–I; component wise (a) J_X and (b) J_Y (A/m). Colour scale indicates: red strongest and blue weakest.

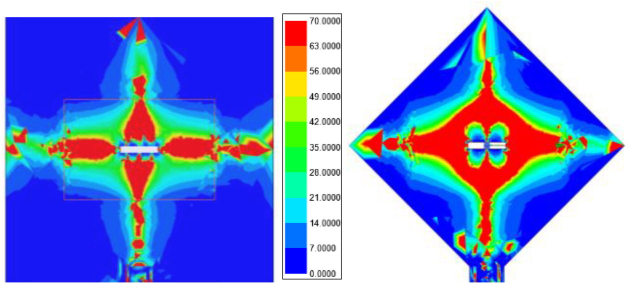

(a) (b)

FIGURE 4. Magnitude portrays of J_X/J_Y on ground plane for (a) conventional; (b) GP configuration – I. Red indicates strongest and blue is weakest fields.

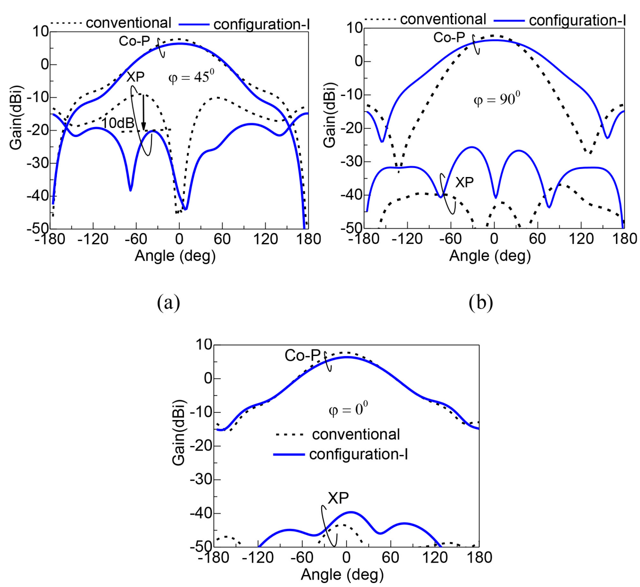

FIGURE 5. Simulated gain patterns of the proposed antenna with proposed GP configuration-I at f_r = 2.92GHz compared with the conventional square ground at resonance frequency f_r = 2.95GHz (a) D-plane, (b) H-plane, (c) E-plane.

(*b*) Adequate 'Low J_Y' (observed in Fig. 1 (b)) is maintained in Fig. 3(b).

A more indicative result is shown in Fig. 4 which compares the change in J_X/J_Y ratio and ensures improved J_X/J_Y

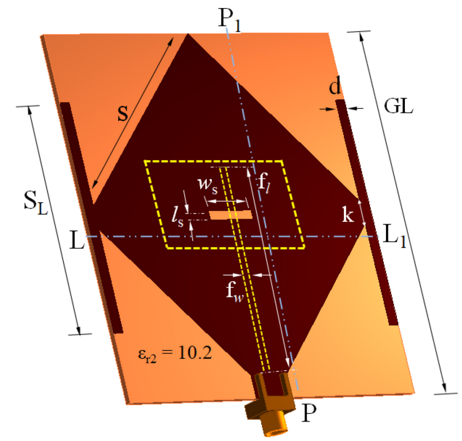

FIGURE 6. Schematic view of modified ground: GP configuration-II with variable S_L. Parameters as in Table 2.

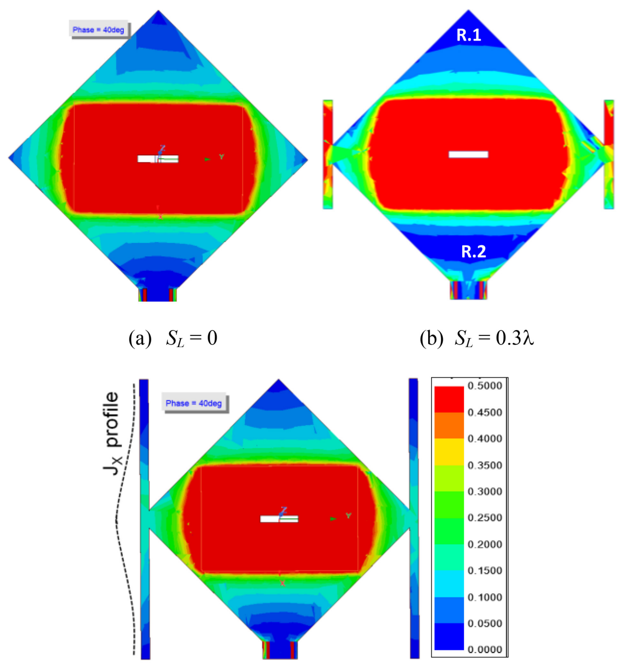

(c) $S_L = 0.8\lambda$

FIGURE 7. Magnitude portrays of x-polarized conduction current components (J_X A/m) on antenna ground, (a) GP-I ($S_L = 0$), (b) GP-II with $S_L = 0.3\lambda$, and (c) GP-II with $S_L = 0.8\lambda$.

in the proposed configuration. Their impact on the radiation characteristics has been examined in Fig. 5. The peak gain is found to be reduced by about 1.5 dB compared to the reference antenna and this justifies reduction in the effective radiating aperture caused by GP shaping. The H-plane pattern gets noticeably wider due to the same reason. But the most important achievement is its XP suppression over D-planes (Fig. 5(a)). It promises to be around 10dB although an equal order of degradation happens in H-plane (Fig. 5(b)). A tendency of a relative hike is also apparent in the E-plane XP values (Fig. 5(c)). Such XP behavior may be attributed to the improvised J_X and J_Y distributions on GP

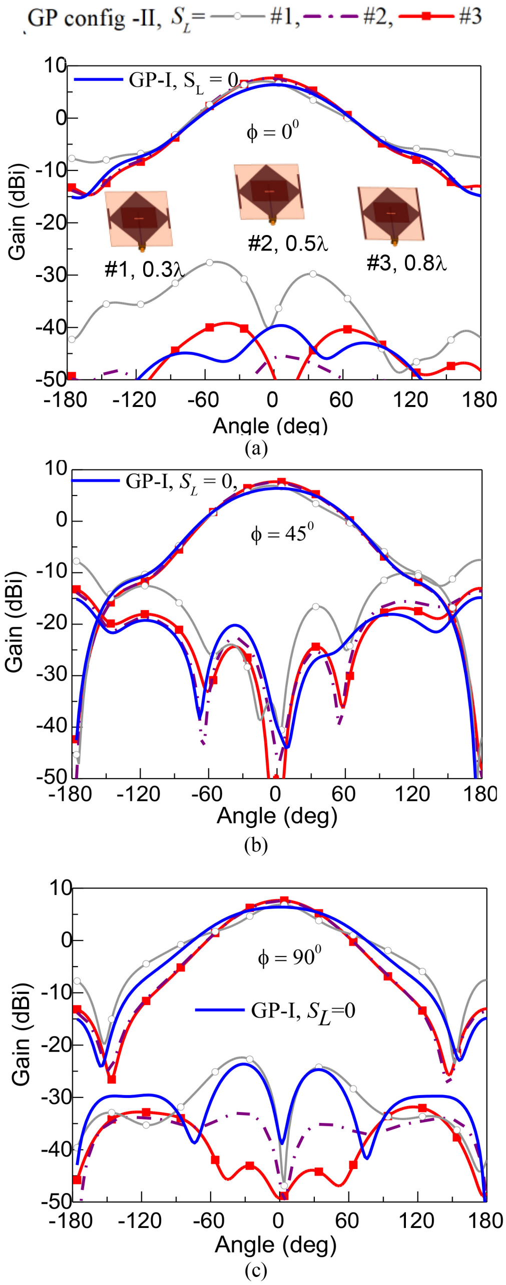

FIGURE 8. Effect of strip length (S_L) over gain pattern is examined in (a) E-plane, (b) D-plane, (c) H-plane. Other parameters as in Table 2.

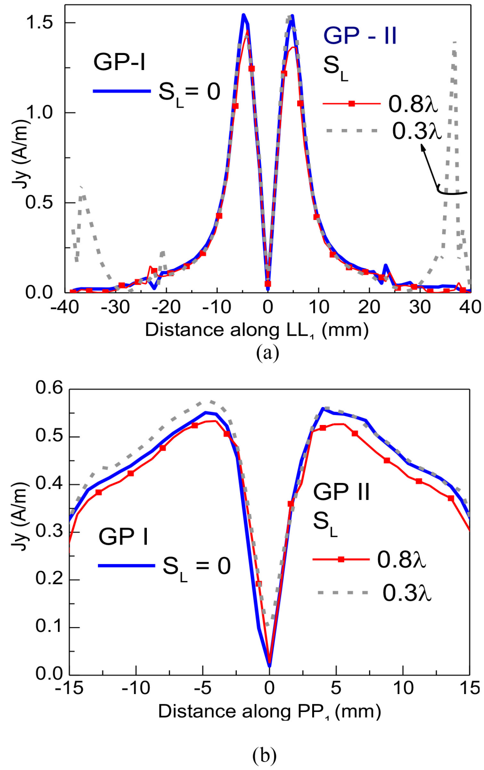

FIGURE 9. Y-polarized current components (J_Y A/m) for various strip length (S_L) extracted across (a) line LL_1, (b) Line PP_1. Other parameters as in Table 2.

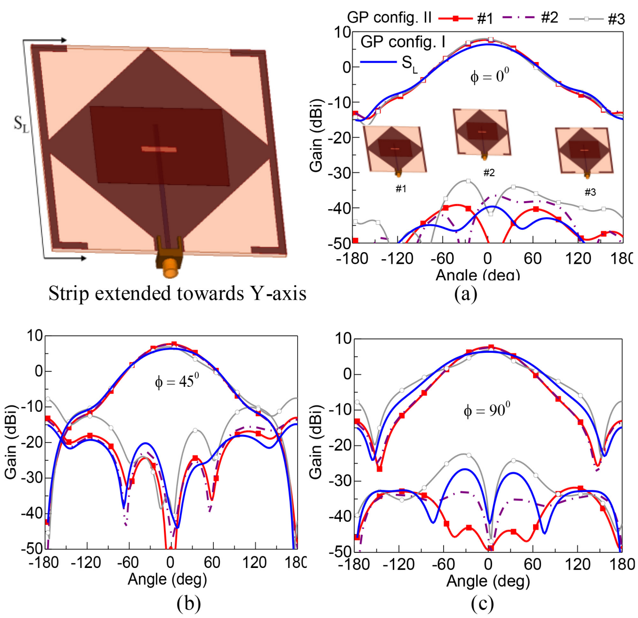

FIGURE 10. Effect of extension of strip length (S_L) along Y-axis over gain as examined for (a) E-plane, (b) D-plane, (c) H-plane.

configuration - I. That complies with our primary goal, i.e., to obtain the lowest possible XP over the D-plane. The new balance in J_X and J_Y however, does not support the most ideal situation (case (iii) in Table 1: maximum J_X with minimum J_Y revealing no degradation in the primary radiation) in producing the lowest XP radiation over E- or H-plane. Those values in aperture-fed patch are inherently low (~ -35dBi) and hence even after some degrees of increment, the XP remains adequately low, say about -28dBi in H and -40dBi in E-planes. Hence, the improvisation as in GP configuration-II does not cause any harm from engineering point of view. Rather it improves the overall XP scenario from the 3D perspective.

But, this trend of increment in E- and H-pane XP is not a healthy indication of the new design. So, in here, a further scope arises to improvise the electrical parameters of

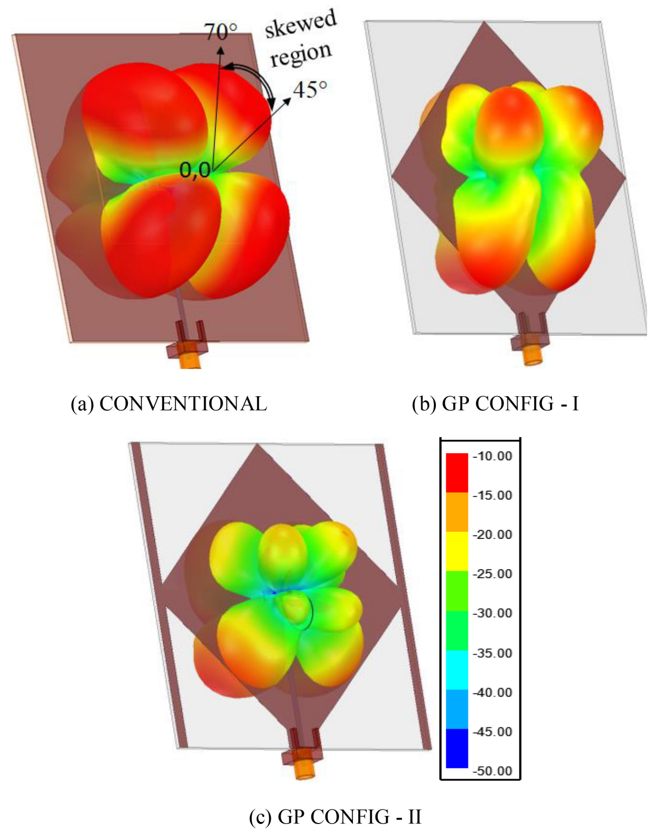

FIGURE 11. 3D visualization of XP radiations for (a) conventional (b) with GP configuration-I, (c) GP configuration-II. Parameters as in Table 2, S_L = 80 mm.

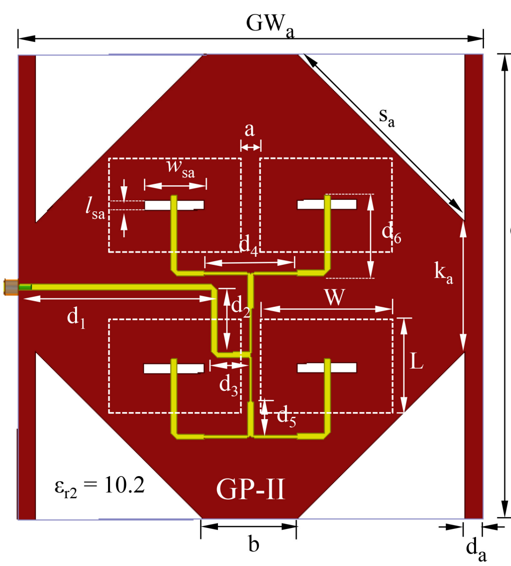

FIGURE 12. Schematic view of proposed 2×2 aperture coupled corporate fed array with GP configuration-II. ε_{r1} = 2.33, ε_{r2} = 10.2, h_1 = 1.575mm and h_2 = 1.27mm Parameters as in Table 2. Patch is shown in dotted line.

the proposed antenna in favor of lower XP fields in both D-and H-planes. The following section embodies investigation focusing on this aspect and proposes another modified version of GP.

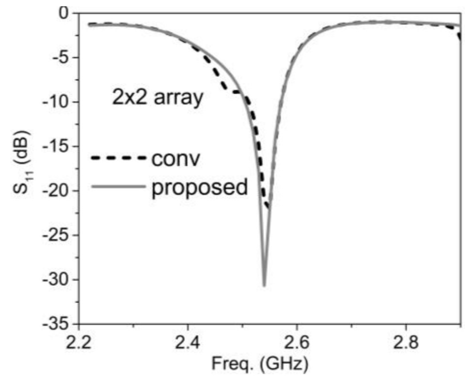

FIGURE 13. Simulated S_{11} characteristics for the proposed and conventional array. Parameters as in Fig. 12 and Table 2.

B. GP CONFIGURATION-II

The aim of this whole investigation is to enhance x-polarized current but at the same instance the configuration-I should remain unperturbed. A pair of thin metal strips of variable length S_L as shown in Fig. 6 has been introduced. We prefer to call it as ‘GP Configuration-II’. Its impact on overall J_X as a function of S_L dimension has been examined in Fig. 7. GP-II with $S_L = 0$ degenerates to GP-I (Fig. 8(a)). As S_L is increased to $S_L \approx 0.3\lambda$, the GP area containing weak J_X increases (region R.1, R.2 as shown in Fig. 8(b)). At the same time, J_X concentrates on the narrow strips. But with $S_L \approx 0.8\lambda = \text{GL}$ (Fig. 8 (c)), J_X regains its distribution over relatively larger area. Its impact has been studied in Fig. 9. The full-length S_L ($\approx 0.8\lambda$= GL) appears relatively improved compared to other versions bearing $S_L <$ GL. GP-II is larger in size compared to GP-I and that is manifested through an increment in peak gain by about 1.5 dB and narrowing down the H-plane pattern.

One may notice in Fig. 8 that both D- and H-plane XP levels drastically increase when the newly introduced $S_L \approx 0.3\lambda$. As per Table 1, condition (ii), increase in J_Y might be a reason behind this. This has been cross verified in Fig. 10. Parameter J_Y has been compared across two arbitrary lines LL_1 & PP_1 (on Fig. 6) and they are plotted in Fig. 9. The case $S_L \approx 0.3\lambda$ indicates a sharp rise in J_Y over LL_1 and a nominal rise over PP_1.

A further increase in S_L as shown in Fig. 10(a) is also possible but that does not help in achieving our goal; both H- and D-plane XP values become worse as shown in Figs. 10 (b, c). Thus, GP-II with S_L = GL appears to be the best choice and its XP performance compared to that in GP-I and a conventional reference patch has been shown in Fig. 11. The simulated portrays indeed (Fig. 11) help in visualizing the degree of 3D relative suppression by GP-II. As a result, we limited the rest of our investigations to GP configuration-II exclusively.

IV. DESIGN FEASIBILITIES IN ARRAYS

The studies so far were focused to a standalone patch on GP config-II ensuring its utility in reducing the overall XP level

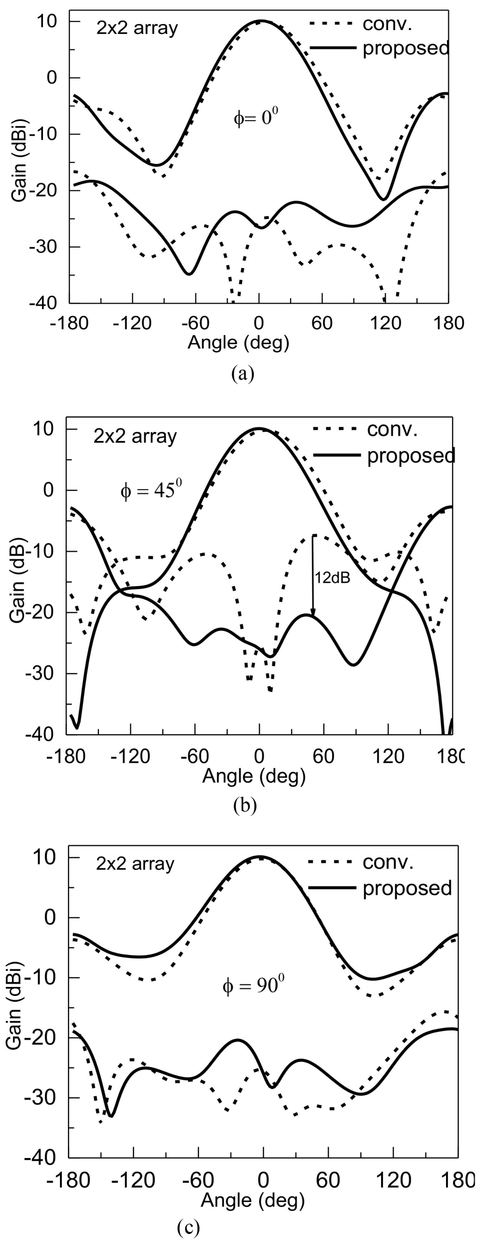

FIGURE 14. Simulated gain of the proposed array in (a) E-plane, (b) D-plane, (c) H-plane. Conventional pattern is also included for comparison. Parameters are as in Fig. 12 and Table 2.

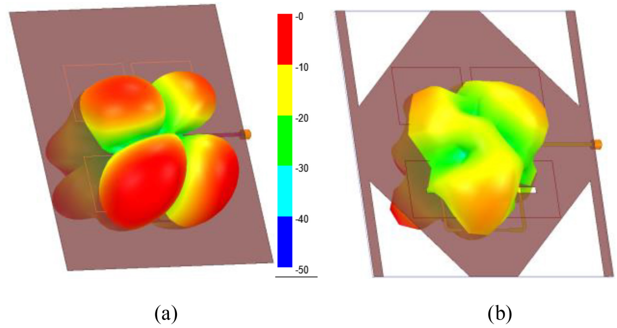

FIGURE 15. Simulated 3-D visualization of XP radiations for (a) conventional; (b) proposed array bearing GP configuration-II. Parameters as in Fig. 14.

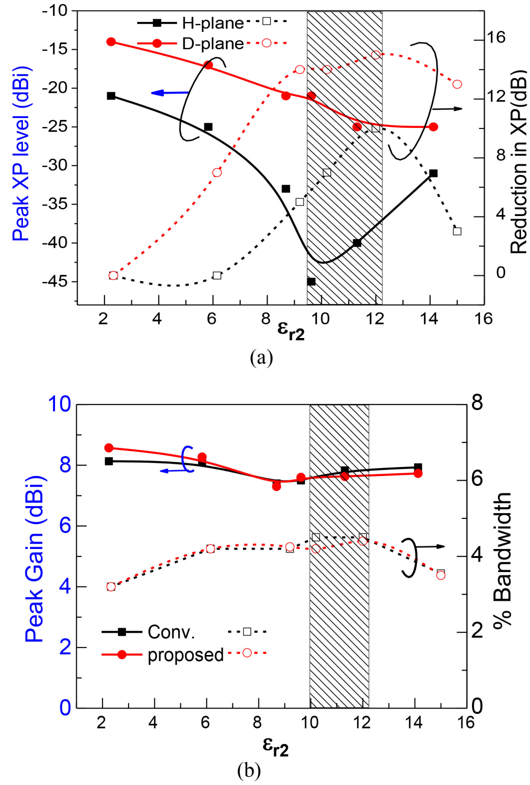

FIGURE 16. Antenna characterization for both conventional and proposed structure (configuration-II) in terms of varying ε_{r2}: (a) absolute XP level and its relative reduction compared to a conventional geometry; (b) peak gain and impedance bandwidth. Other parameters as in Table 2, ε_{r1} = 2.33.

encompassing both diagonal and orthogonal planes. Whether the same GP-II is equally applicable to array configuration is examined in this section. A 2×2 array of identical patches (Fig. 12) indicates almost no change in S_{11} characteristics with respect to its conventional version as shown in Fig. 13. But as predicted, the XP radiations get significantly reduced in D- plane as shown in Fig. 14. Over the H- and E-plane, the XP values show no noticeable relative changes. Thus, about 10 dB suppression in D-plane eventually results in uniform cross-polar discrimination over entire 3D patterns by nearly 30dB. This scenario can be visualized from the simulated portray of the same as depicted in Fig. 15. In a color diagram, 'red' indicates the strongest and 'blue' indicates is weakest radiation and thus the figure is self-explanatory. The strip loaded rhombic GP is also successfully suppressing the XP radiations across the entire azimuth plane (φ).

V. IMPACT OF ANTENNA PARAMETERS: POSSIBLE DESIGN VARIATION

An engineering aspect of the proposed design using a range of commercially available PTFE substrates has been critically studied. Substrate permittivity ε_{r2} for the feed line has been

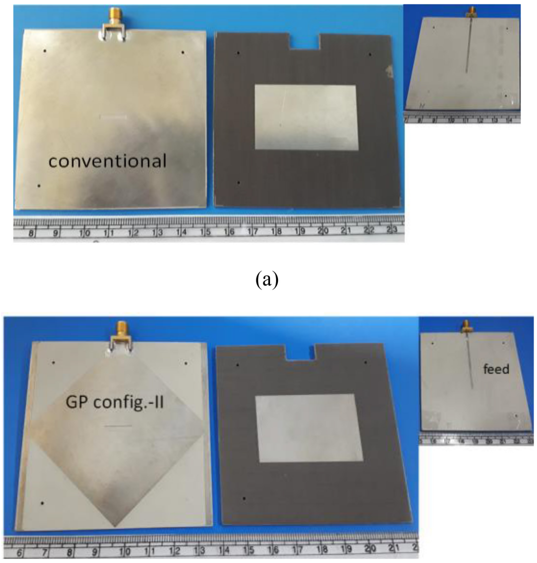

(a)

(b)

FIGURE 17. **Photographs of the prototypes (Layered view): (a) conventional aperture fed patch, (b) proposed GP configuration - II. Parameters as $l_P = 30$, $w_P = 45$, h = 1.575, $\varepsilon_{r1} = 2.33$, $\varepsilon_{r1} = 10.2$, k = 5, $f_l = 50$, $f_w = 1.5$, d = 2.5, GL = GW = S_L = 80 (all dimensions in mm). Inset: image of feed line.**

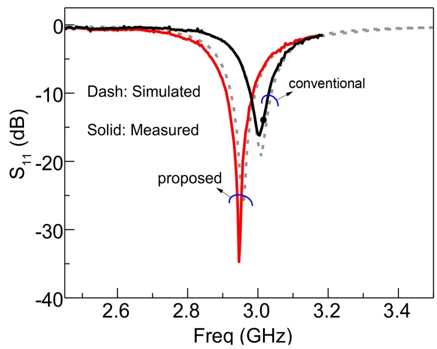

FIGURE 18. **Measured S_{11} of the proposed and conventional prototypes compared with simulated predictions. Parameters as in Fig. 17.**

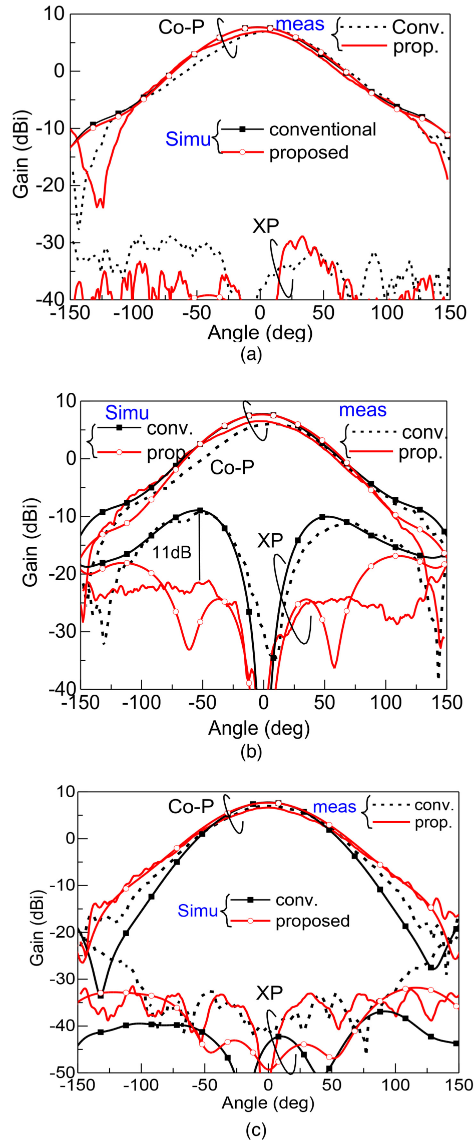

FIGURE 19. **Measured radiation patterns obtained at f = 3.08GHz (conventional), 2.92GHz (proposed), compared with simulated predictions. (a) E-plane, (b) D-plane, (c) H-plane. Parameters as in Fig. 18.**

varied, keeping that for the microstrip element unchanged. As indicated by the plots in Fig. 16 (a), the peak XP levels (for both H- and D-planes) decrease with an increase in ε_{r2} values up to a certain minima and then rise up.

It is important to note that the lowest possible XP values are closely associated with the maximum order of XP suppression as highlighted by a shaded area. The optimum results are revealed with ε_{r2} ranging from 9.5 to 12.2 for the present study. But its impact on the bandwidth and gain as examined in Fig. 16(b) does not appear so significant. It, therefore, seems that the relative dielectric constant of the bottom substrate has to be restricted within the range of 10 to 12 to guarantee the lowest possible XP with highest possible reduction.

VI. PROTOTYPES AND EXPERIMENTAL RESULTS

A set of S-band prototypes, each being split in two units, are shown in Fig. 17. The final design using the proposed configuration-II has been compared with a conventional counterpart. The feed line unit for aperture coupled patch is shown as inset. They were measured using E8363B network analyzer and an automated anechoic chamber. Fig. 18 compares the measured S_{11} values with simulated predictions for both conventional and config.-II types. Excellent mutual agreement is revealed.

The proposed antenna experiences a little left shift in resonance which perhaps is caused by some inductive loading through redistributed conduction current.

Their radiation characteristics along with respective simulated predictions are examined in Fig. 19. The measurement setup allows capturing reliable data up to 150° azimuth plane. The co-pol patterns closely follow the simulated predictions and indicate no major change in gain

TABLE 3. Proposed design compared with other contemporary works based on measured data.

Some Reported Works: Category	Some Reported Works: Configurations	Operating Frequency	Type of feed	H-plane XPD isolation (dB)	D-plane XPD isolation (dB)	Peak Gain (dBi)	Physical Size ($l \times w \times h$) in λ_0	REMARKS (Profile/ Design complexity/ Sensitivity etc.)
Pole/pin loaded structure	Non-planar vertical loading [16], [17]	S-band	probe	18	11	7.5	1×1×0.12 (0.25)*	Tall, easy to fabricate, unchanged antenna gain
		X-band		19	Not addressed	8.2	1×1×0.12(0.25)*	
	Dual-feed capacitive fence [31]	S-band	Probe	20	Not addressed	6	1.4×1.4×0.07	Compact, multi-parametric, challenging fabrication in higher frequency
	Shorted pin grooved patch [15]	S-band	probe	21	Not addressed	6	0.9×0.9×0.015	Standalone patch, No D-plane value
Differential Feed	Hybrid Feed & Slot Loaded Dual-polarized array[24]	S-band	probe	36	$30^{\$,\#}$	(i)No data (single) (ii) 20 (6×6)	0.5×0.5×0.07 (single elem.)	Well port isolation and XPD Complex Feed network
	UWB microstrip [32]	S-X band	Microstrip	20-28	Not addressed	3-5	0.8×0.6×0.015	Wide bandwidth, compact size, single element
	Microstrip in [33]	S-band	Aperture	35	Not addressed	7.5	-	Wideband, low XP, No D-plane value
GP engineering / Defects	DGS technique [10]	X-Ku band	Probe	15-20	Not addressed	6.5	1.66×1.66×0.083	Wideband, Planar, ground slot increase back radiation and may reduce peak gain, slots are constraint for array
	Engineered GP [19], [21]	S-band	Probe	20	16	7.5	0.8×0.8×0.012	
		C-band	Microstrip	23 (single) 28 (array)#	19(single) 17(array)#	7.8 13	1.04×1.04×0.015 2.14×1.77×0.015	
	'W'/ 'step'- shaped GP [13], [14]	S/L-band	probe	13 18	Not addressed	9.4 -	0.8×1×0.45 ($\pi 1.73^2$)×0.26	Bulky ground, volumnous structure
	Proposed GP config. - II with (i) Single element (ii) 2x2 array	**S-band**	**Aperture**	**31(single) 32 (array)**	**27 (single) 32 (array)**	**7.8 10**	**0.8×0.8×0.026 1.2×1.2×0.026**	**Planar, applicable in array, No additional engineering required**

*: smaller variant #: simulated, $: scanning angle 45^0

and beamwidth compared to the conventional geometry. Reduction in D-plane XP level by about 11dB is ensured by the measured data, but the dips around ±55° present in the simulated XP pattern is found to be absent. Some degree of misalignment especially for D-plane measurement may be attributed to this. Measured H-plane XP values, as predicted by the simulated data, remain comparable with the conventional case, and they appear below −30dB. It ensures peak to peak co-to-cross-polar isolation about 34 dB in H-plane. E-plane XP level is identical with the H-plane values and thus, our proposed configuration II experimentally promises over 26dB co-to-cross-polar isolation in 3D scenario. A comprehensive comparison with the earlier investigations is presented in Table 3 which has been discussed later in conclusion section.

VII. CONCLUSION

The design is straightforward, low cost, commercially viable, and easy to implement. It, for the first time, shows how a strategic perturbation causes minimal removal of effective ground plane that results in no loss in gain. This indeed is one of the major advantages compared to earlier DGS based D-plane XP reduction techniques [19], [20], [21]. The proposed design does not require any additional hardware or critical machining. It, therefore, should support both standalone patch and planar arrays effectively in terms of improved polarization purity over the entire radiation planes.

A comprehensive comparison with a set of earlier representative designs has been documented in Table 3. Very few of them addressed D-plane properties. The major advantage is its ability in accommodating corporate feed networks which was noticeably missing in the earlier investigations. Our proposed approach appears relatively improved and commercially viable compared to all of those.

ACKNOWLEDGMENT

The authors thankfully acknowledge the useful comments made by the review board and also the technical help received from their group member Sk Rafidul at the University of Calcutta.

REFERENCES

[1] R. Hansen, "Cross polarization of microstrip patch antennas," *IEEE Trans. Antennas Propag.*, vol. 35, pp. 731–732, Jun. 1987.

[2] T. Huynh, K. F. Lee, and R. Q. Lee, "Crosspolarisation characteristics of rectangular patch antennas," *Electron. Lett.*, vol. 24, no. 8, pp. 463–464, Apr. 1988.

[3] K. F. Lee, K. M. Luk, and P. Y. Tam, "Cross polarization characteristics of circular patch antenna," *Electron. Lett.*, vol. 28, no. 6, pp. 587–589, Mar. 1992.

[4] M. L. Oberhart, Y. T. Lo, and R.Q. H. Lee, "New simple feed network for an array module of four microstrip elements," *Electron. Lett.*, vol. 23, no. 9, pp. 436–437, Apr. 1987.

[5] J. Huang, "Dual-polarised microstrip array with high isolation and low cross-polarization," *Microw. Opt. Technol. Lett.*, vol. 4, no. 3, pp. 99–103, Feb. 1991.

[6] D. Dutta and D. Guha, "Composite shorted patch designed for improved radiation patterns," in *Proc. IEEE Indian Conf. Antennas Propag. (InCAP)*, Ahmedabad, India, 2019, pp. 1–3.

[7] G. Xu, H.-L. Peng, Z. Shao, L. Zhou, Y. Zhang, and W.-Y. Yin, "Dual-band differential shifted-feed microstrip grid array antenna with two parasitic patches," *IEEE Trans. Antennas Propag.*, vol. 68, no. 3, pp. 2434–2439, Mar. 2020.

[8] Y. J. Sung and Y.-S. Kim, "An improved design of microstrip patch antennas using photonic bandgap structure," *IEEE Trans. Antennas Propag.*, vol. 53, no. 5, pp. 1799–1804, May 2005.

[9] F. Yang and Y. Rahmat-Samii, *Electromagnetic Band Gap Structures in Antenna Engineering*. Cambridge, U.K.: Cambridge Univ. Press, 2009.

[10] T. Sarkar, A. Ghosh, L. L. K. Singh, S. Chattopadhyay, and C.-Y.-D. Sim, "DGS-integrated air-loaded wideband microstrip antenna for X- and Ku-band," *IEEE Antennas Wireless Propag. Lett.*, vol. 19, no. 1, pp. 114–118, Jan. 2020.

[11] F. Y. Zulkifli, E. T. Rahardjo, and D. Hartanto, "Radiation properties enhancement of triangular patch microstrip antenna array using hexagonal defected ground structure," *Progr. Electromagn. Res. Mag.*, vol. 5, pp. 101–109, Jan. 2008.

[12] D. Guha, C. Kumar, and S. Biswas, *Defected Ground Structure (DGS) Based Antennas: Design Physics, Engineering and Application*, 1st ed. Hoboken, NJ, USA: Wiley-IEEE Press, 2022, ch. 5.

[13] W. H. Hsu and K. L. Wong, "Broad-band probe-fed patch antenna with a 'U-shaped' ground plane for cross-polarization reduction'," *IEEE Trans. Antennas Propag.*, vol. 50, no. 3, pp. 352–355, Mar. 2002.

[14] K. L. Wong, C. L. Tang, and J. Y. Chiou, "Broadband probe-fed patch antenna with a W-shaped ground plane," *IEEE Trans. Antennas Propag.*, vol. 50, no. 6, pp. 827–831, Jun. 2002.

[15] N.-W. Liu, L. Zhu, Z.-X. Liu, Z.-Y. Zhang, G. Fu, and Y. Liu, "Cross-polarization reduction of a shorted patch antenna with broadside radiation using a pair of open-ended stubs," *IEEE Trans. Antennas Propag.*, vol. 68, no. 1, pp. 13–20, Jan. 2020.

[16] D. Dutta, D. Guha, and C. Kumar, "Mitigating unwanted mode in a microstrip patch by a simpler technique to reduce cross-polarized fields over the orthogonal plane," *IEEE Antennas Wireless Propag. Lett.*, vol. 20, no. 5, pp. 678–682, May 2021.

[17] D. Dutta, D. Guha, and C. Kumar, "Microstrip patch with grounded spikes: A new technique to discriminate orthogonal mode for reducing cross-polarized radiations," *IEEE Trans. Antennas Propag.*, vol. 70, no. 3, pp. 2295–2300, Mar. 2022.

[18] S. Bhardwaj and Y. Rahmat-Samii, "Revisiting the generation of cross-polarization in rectangular patch antennas: A near-field approach," *IEEE Antennas Propag. Mag.*, vol. 56, no. 1, pp. 14–38, Feb. 2014.

[19] D. Dutta, S. Rafidul, D. Guha, and C. Kumar, "Suppression of cross-polarized fields of microstrip patch across all skewed and orthogonal radiation planes," *IEEE Antennas Wireless Propag. Lett.*, vol. 19, no. 1, pp. 99–103, Jan. 2020.

[20] M. I. Pasha, C. Kumar, and D. Guha, "Mitigating high cross-polarized radiation issues over the diagonal planes of microstrip patches," *IEEE Trans. Antennas Propag.*, vol. 68, no. 6, pp. 4950–4954, Jun. 2020.

[21] S. Rafidul, D. Guha, and C. Kumar, "Sources of cross-polarized radiation in microstrip patches: Multiparametric identification and insights for advanced engineering," *IEEE Antennas Propag. Mag*. vol. 65, no. 2, pp. 92–103, Apr. 2023, doi: 10.1109/MAP.2022.3143434.

[22] D. M. Pozar, "Microstrip antenna aperture-coupled to a microstripline," *Electron. Lett.*, vol. 21, no. 2, pp. 49–50, Jan. 1985.

[23] P. Sullivan and D. Schaubert, "Analysis of an aperture coupled microstrip antenna," *IEEE Trans. Antennas Propag.*, vol. 34, no. 8, pp. 977–984, Aug. 1986.

[24] H. Saeidi-Manesh and G. Zhang, "High-isolation, low cross-polarization, dual- polarization, hybrid feed microstrip patch array antenna for MPAR application," *IEEE Trans. Antennas Propag.*, vol. 66, no. 5, pp. 2326–2332, May 2018.

[25] Y. Wang and V. Chandrasekar, "Polarization isolation requirements for linear dual-polarization weather radar in simultaneous transmission mode of operation," *IEEE Trans. Geosci. Remote Sens.*, vol. 44, no. 8, pp. 2019–2028, Aug. 2006.

[26] N. A. Aboserwal, J. L. Salazar, J. A. Ortiz, J. D. Díaz, C. Fulton, and R. D. Palmer, "Source current polarization impact on the cross-polarization definition of practical antenna elements: Theory and applications," *IEEE Trans. Antennas Propag.*, vol. 66, no. 9, pp. 4391–4406, Sep. 2018.

[27] C. A. Balanis, *Antenna Theory: Analysis and Design*, 3rd ed. New York, NY, USA: Wiley, 2005.

[28] A. K. Bhattacharyya, "Effects of finite ground plane on the radiation characteristics of a circular patch antenna," *IEEE Trans. Antennas Propag.*, vol. 38, no. 2, pp. 152–159, Feb. 1990.

[29] A. C. Ludwig, "The definition of cross polarization," *IEEE Trans. Antennas Propag.*, vol. AP-21, no. 1, pp. 116–119, Jan. 1973.

[30] *High Frequency Structure Simulator (HFSS) V. 2022 R1*, ANSYS, Pittsburgh, PA, USA, 2022.

[31] Y. He and Y. Li, "Dual-polarized microstrip antennas with capacitive via fence for wide beamwidth and high isolation," *IEEE Trans. Antennas Propag.*, vol. 68, no. 7, pp. 5095–5103, Jul. 2020.

[32] J. Wang and Y. Yin, "Differential-fed UWB microstrip antenna with improved radiation patterns," *Electron. Lett.*, vol. 50, no. 20, pp. 1412–1414, Sep. 2014.

[33] C. H. Lai, T. Y. Han, and T. R. Chen, "Broadband aperture-coupled microstrip antennas with low cross polarization and back radiation," *Prog. Electromag. Res. Lett.*, vol. 5, pp. 187–197, Jan. 2008.

DEBI DUTTA (Graduate Student Member, IEEE) was born in West Bengal, India. She received the B.Tech. and M.Tech. degrees in radio physics and electronics from the University of Calcutta, India, in 2015 and 2017, respectively, where she is currently pursuing the Ph.D. degree with the Institute of Radio Physics and Electronics.

Her current research interests include planar and non-planar antennas for space-borne and mobile applications, cross-polar discriminations in microstrip radiators and solutions for high isolation over 3-D radiation planes.

Dr. Dutta was a recipient of the C. J. Reddy Best Young Professional Award in IEEE InCAP Conference 2018, Bengaluru, and Antenna and Propagation Society Ph.D. travel grant in IEEE AP-S/URSI 2021 Conference, Singapore. She has been nominated as an Outstanding Student Volunteer by the IEEE AP/MTT-s Kolkata Chapter twice in 2021 and 2022. She was the Chair and the Vice-Chair of IEEE APS Student Branch Chapter, Calcutta University from 2020 to 2022 and from 2019 to 2020, respectively. She is currently volunteering as a Student Representative of IEEE AP/MTT-s Kolkata Chapter, Kolkata, India. She is an Active Volunteer of the IEEE.

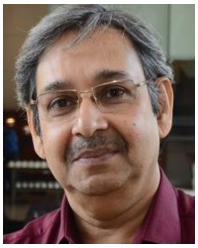

DEBATOSH GUHA (Fellow, IEEE) received the B.Tech. degree in 1987, the M.Tech. degree in 1989, and the Ph.D. degree in microwave engineering from the University of Calcutta.

Then, he joined the University of Calcutta as an Assistant Professor in 1994. Later on, he spent about a couple of years with the Royal Military College of Canada, Kingston, ON, Canada, as a Visiting Research Professor. He is a Professor of Radio Physics and Electronics with the University of Calcutta. He is also an Adjunct Professor with the Malaviya National Institute of Technology Jaipur, India. He started his career in a Telecommunication Industry in India. He is a Fellow of all four Indian National Academies for Science and Engineering, e.g., Indian National Science Academy; the Indian Academy of Sciences, Bengaluru; The National Academy of Sciences, Allahabad, India; and the Indian National Academy of Engineering. He has researched in developing microstrip and dielectric resonator antenna technologies. Defected ground structure-inspired antenna is one of his major areas of contribution. More than 200 technical papers in IEEE journals and conferences along with a couple of books on planar antenna published by IEEE Press/Wiley are to his credit. Several of his invented techniques are now commonly used by industries and the leading R&D Labs. A novel high gain wireless antenna developed by him has been a commercial product since 2007 in the North American market. He has mentored more than 23 doctoral and postdoctoral students over the last two decades. His current research interests include defected ground structure and metasurface induced antenna, hybrid sub-array structures, solving cross-polarization issues for SAR, and advanced resonance cavity antenna techniques.

Prof. Guha is a recipient of some notable awards which include IETE Ram Lal Wadhwa Award in 2016, Raj Mittra Travel Grant Award in 2012, URSI Young Scientist Award in 1996, and Jawaharlal Nehru Memorial Fund Prize in 1984. He served as an Associate Editor for IEEE TRANSACTIONS ON ANTENNAS AND PROPAGATION and IEEE ANTENNAS AND WIRELESS PROPAGATION LETTERS. He has been currently serving the IEEE AP-S AdCom as the Chair of AP-S Member and Geographic Activities Committee and the Co-Chair of the AP-S Technical Committee on Antenna Measurements. He is a Co-Founder of a leading conference MAPCon (IEEE Microwaves Antennas and Propagation Conference) in India initiated in 2022. Prior to MAPCon, he conceptualized and established IEEE Applied Electromagnetics Conference in 2007 as a major biennial IEEE meeting in India and IEEE Indian Antenna Week as a yearly international workshop in 2010. He has been serving as the Indian Chair of URSI Commission B and the Representative of the Indian National Committee for URSI since 2014. He served as the Chair of the IEEE Kolkata Section from 2013 to 2014 and the Founding Chair of AP/MTT-S Kolkata Chapter in 2004. He served as a member of IEEE AP-S Fields Award Committee from 2017 to 2019. He is an Abdul Kalam Technology Innovation National Fellow.

CHANDRAKANTA KUMAR (Senior Member, IEEE) received the M.Tech. and Ph.D. degrees in radio physics and electronics from the University of Calcutta, India, and completed Space Studies Program from International Space University, Strasbourg, France.

He joined Communication Systems Group, U R Rao Satellite Centre, ISRO, Bengaluru, in 2001. He has designed antenna systems of about twenty spacecrafts, including Mars Orbiter Mission, Chandrayaan-1 and 2, Moon Impact Probe. He also worked for the ground stations like 32-m diameter "Indian Deep Space Network Station" IDSN-32, satellite tracking antennas, and transportable tracking terminals. He served as the Deputy Project Director for RF Systems of Chandrayaan-2 Orbiter; and the Project Manager for antenna systems of Chandrayaan-1, Moon Impact Probe, and ASTROSAT and GSAT-12 missions. He has 145 technical publications, including 55 in IEEE journals/magazines to his credit and has supervised two Masters' and three Ph.D. theses. He is a Fellow of the Indian National Academy of Engineering, the West Bengal Academy of Science and Technology, and the Institution of Electronics and Telecommunication Engineers. His present research areas are low cross-pol antennas, microwave photonic techniques, lightweight phased array antennas, and RF systems for spacecrafts.

Dr. Kumar is a recipient of "Young Scientist Merit Award-2009" and "Team Excellence Award-2008" from ISRO, and "Prof. S. N. Mitra Memorial Award-2011" and Hari Ramji Toshniwal Award-2018 from IETE, India. He also received 2*nd* Best Paper Award in InCAP 2019, Ahmedabad; the second and third Best Paper Awards in iAIM-2017, "K U Limaye" Memorial Best Paper Awards in ISM-2008 and IRSI 2009 held in Bengaluru. He is currently serving as an Associate Editor for IEEE ANTENNAS AND WIRELESS PROPAGATION LETTERS and is on the board of reviewers of IEEE TRANSACTIONS ON ANTENNAS AND PROPAGATION, *IEEE Antennas and Propagation Magazine*, and *IET Microwaves, Antennas & Propagation*. He is currently the Vice Chair of the Bangalore Section and the Chair-Elect of its AP-MTT joint chapter. He was the TPC and the Publication Chair of inaugural edition of B-HTC 2020 and served as the Organizing Chair of CONECCT-2021, 2022, and 2023 conferences of Bangalore Section. He is an Active Volunteer of IEEE.